Journal of Molecular Catalysis A: Chemical 355 (2012) 186–191

Contents lists available at SciVerse ScienceDirect

Journal of Molecular Catalysis A: Chemical

journal homepage: www.elsevier.com/locate/molcata

Novel homogeneous catalyst comprising ruthenium and trimethylphosphite for the hydrolysis of sodium borohydride

Mehdi Masjedi[a], Leyla Tatar Yildirim[b], Saim Özkar[a,*]

[a] Department of Chemistry, Middle East Technical University, 06531 Ankara, Turkey
[b] Department of Engineering Physics, Hacettepe University, 06800 Ankara, Turkey

ARTICLE INFO

Article history:
Received 21 August 2011
Received in revised form 8 December 2011
Accepted 9 December 2011
Available online 17 December 2011

Keywords:
Ruthenium
Trimethylphosphite
Sodium Borohydride
Hydrolysis
Homogeneous catalysis

ABSTRACT

Homogeneous catalytic hydrolysis of sodium borohydride starting with $Ru(acac)_3$ (acac = acetylacetonate) and $P(OMe)_3$ was followed by monitoring the hydrogen evolution and the UV–vis electronic absorption spectra which shows the conversion of all ruthenium(III) to a ruthenium(II) species, most likely acting as catalyst. This active catalyst is alive only under reducing conditions and converted mainly to $Ru(acac)_3$ along with other minor complexes when the catalytic reaction is over. A ruthenium(II) complex was isolated from the reaction solution after the complete catalytic hydrolysis of sodium borohydride and characterized to be $[Ru\{P(OMe)_3\}_4H_2]$ by single crystal XRD, MS, UV–vis, FTIR, ^1H, ^{13}C and ^{31}P NMR spectroscopy. $[Ru\{P(OMe)_3\}_4H_2]$ complex crystallizes in the triclinic space group P-1 with $a = 10.066(2)$ Å, $b = 19.108(3)$ Å, $c = 20.938(4)$ Å, $\alpha = 78.839(14)^\circ$, $\beta = 87.308(16)^\circ$ and $\gamma = 79.506(14)^\circ$. This ruthenium(II) complex was found not to be the active catalyst in the hydrolysis of sodium borohydride, rather one of its conversion products after catalysis. Although the active catalyst could not be isolated from the reaction solution, it could be stabilized by adding chelating 2,2′-bipyridine into the solution during the catalysis. Thus, a stabilized form of the active catalyst, $[Ru(acac)(bipy)\{P(OMe)_3\}H]$, could be isolated and characterized by MS, UV–vis, FTIR, ^1H, ^{13}C and ^{31}P NMR spectroscopy. $[Ru(acac)(bipy)\{P(OMe)_3\}H]$ is expectedly not as active as the ruthenium(II) species formed in situ during the catalysis. Taking all the results together reveals that the active catalyst is a ruthenium(II) complex, either $[Ru(acac)\{P(OMe)_3\}_3H]$ or most likely its dissociation product, $[Ru(acac)\{P(OMe)_3\}_2H]$. Control experiments showed that 2,2′-bipyridine can replace only the trimethylphosphite ligands but not the acetylacetonato ligand in the ruthenium(II) complex.

1. Introduction

A recent study [1] has shown that ruthenium(III) acetylacetonate ($Ru(acac)_3$, **1**) acts as homogeneous catalyst at room temperature in hydrogen generation from the hydrolysis of sodium borohydride ($NaBH_4$, SB) in H_2O–THF solution, which has been considered as solid hydrogen storage materials [2–7]. It has also been shown that when trimethylphosphite $P(OCH_3)_3$ is added to the reaction solution containing $NaBH_4$ and **1**, the hydrogen generation was practically stopped (or reduced to the level of self hydrolysis) indicating that the hydrolysis of SB in the presence of **1** is a homogeneous catalysis [8]. However, the catalytic hydrolysis of SB restarts at an unexpectedly high rate in a certain period (induction time) after addition of trimethylphosphite. Accordingly, phosphorus ligand, known to be a poison in the catalysis, is involved in the formation of a new ruthenium species (**2**) containing trimethylphosphite, which has higher catalytic activity in comparison to **1** alone. The rate of hydrolysis varies very slightly with the mole ratio of phosphorus to ruthenium [8]. In other words, changing the mole ratio of $P(OMe)_3$ to **1** in the range of 1–4 does not affect the mechanism of reaction or the structure of active catalyst formed during hydrolysis of SB. Nevertheless, the phosphorus to ruthenium molar ratio of **2** shows slightly higher catalytic activity than the others. Based on this observation, ruthenium(II) acetylacetonato complexes containing two trimethylphosphite ligands have been synthesized and tested as homogeneous catalysts in the hydrolysis of SB [9]. Neither the cis-$[Ru(acac)_2\{P(OMe)_3\}_2]$ nor the trans-$[Ru(acac)_2\{P(OMe)_3\}_2]$ complex, isolated from the reaction of cis-$[Ru(acac)_2(\eta^2\text{-cyclooctene})_2]$ with $P(OMe)_3$ [10,11], has shown any significant activity in the hydrolysis of SB. However, the catalytic activity of cis-$[Ru(acac)_2\{P(OMe)_3\}_2]$ has been shown to be significantly enhanced by addition of 2 equiv. of trimethylphosphite per ruthenium into the medium [9]. This result implies that the catalytically active ruthenium species formed during the hydrolysis of SB starting with **1** and $P(OMe)_3$, most likely, involves more than two phosphine ligands. However, the

* Corresponding author. Tel.: +90 312 210 3212; fax: +90 312 210 3200.
E-mail address: sozkar@metu.edu.tr (S. Özkar).

1381-1169/$ – see front matter © 2011 Elsevier B.V. All rights reserved.
doi:10.1016/j.molcata.2011.12.015

identification of the catalytically active species formed in the hydrolysis of SB starting with **1** and $P(OMe)_3$ in aqueous solution has remained as a challenge in this homogeneous catalysis. Herein we report the results of our further efforts to identify the active catalyst. In particular, we report the isolation of a ruthenium complex, dihydridotetrakis(trimethylphosphite)ruthenium(II), $[Ru\{P(OMe)_3\}_4H_2]$ (**3**), from the aqueous reaction solution during the catalytic hydrolysis of SB starting with **1** and $P(OMe)_3$ and its characterization by single crystal XRD, MS, UV–vis, FTIR, ^1H, ^{13}C, and ^{31}P NMR spectroscopy. The complex **3** could be synthesized via a different route starting with $RuCl_3{\cdot}3H_2O$, $P(OMe)_3$ and $NaBH_4$ in a non-aqueous solution [12]. This ruthenium(II) complex **3** shows some activity in the hydrolysis of SB, though lower than that observed for the in situ generated active species **2**. Since monitoring the UV–vis electronic absorption spectra shows the presence of a ruthenium(II) species in the reaction solution during the catalytic hydrolysis, which seems to be catalytically very active, we attempted to isolate that in situ ruthenium(II) complex either in its active form or in a form stabilized by adding a chelating ligand into solution. Indeed, we could achieve the isolation of a ruthenium(II) complex, $[Ru(acac)(bipy)P(OMe)_3H]$, **4** formed from **2** upon addition of 2,2′-bipyridine (bipy) into the reaction solution. This ruthenium(II) complex **4** was also characterized by MS, UV–vis, FTIR, ^1H, ^{13}C and ^{31}P NMR spectroscopy and found to be less active than **2** in hydrogen generation from the hydrolysis of SB.

2. Experimental

2.1. Materials

Ruthenium(III) acetylacetonate, (97%), sodium borohydride, (98%), trimethylphosphite, and 2,2′-bipyridine were purchased from Aldrich. Tetrahydrofuran and dichloromethane were purchased from Merck. All glassware and Teflon-coated magnetic stir bars were cleaned with acetone, followed by copious rinsing with distilled water before drying at 150 °C in oven for a few hours.

2.2. Equipment

All reactions involving air sensitive compounds were performed under argon or nitrogen atmospheres. ^1H, ^{13}C and ^{31}P NMR spectra were taken on a Bruker Avance DPX 400 MHz spectrometer (400.1 MHz for ^1H; 100.6 MHz for ^{13}C; 161.3 MHz for ^{31}P). Chemical shifts are given in ppm (δ) relative to Me_4Si as internal standard for ^1H, ^{13}C and H_3PO_4 (85% in glass capillary) for ^{31}P NMR. UV–vis electronic absorption spectra were recorded on a Varian Carry-100 double beam spectrometer. The infrared spectra were recorded from KBr pellet using a Bruker AXS Tensor-27 or Vertex 70 ATR/FTIR spectrometer. Positive ion mass spectra were acquired on a Micro TOF-LC/ESI/Ms system.

The experimental setup [13] used for performing the hydrolysis of SB and measuring the hydrogen gas generated from the reaction consists of a 75 mL jacketed reaction flask containing a Teflon-coated stir bar placed on a magnetic stirrer (Heidolph MR-301) and thermostated at 25.0 ± 0.1 °C by circulating water through its jacket from a constant temperature bath (RL6 LAUDA water bath). A graduated glass tube (50 cm in height and 25 mm in diameter) filled with water was connected to the reaction flask to measure the volume of hydrogen gas to be evolved from the reaction.

2.3. Isolation of dihydridotetrakis(trimethylphosphite)ruthenium(II) complex, 3

A stock solution of $P(OMe)_3$ (100 mM) in THF was prepared by dissolving 1.18 mL $P(OMe)_3$ (MW = 124.08 g/mol, d = 1.052 g/mL) to 100 mL THF. For the preparation of catalyst solution with $P(OMe)_3$/**1** ratio of 4, a 4 mL aliquot of the stock solution was diluted to 5 mL by adding THF and, then, 40 mg **1** was added to this solution and dissolved completely by stirring. Then, the solution was transferred into the reaction flask containing 1.2 g (30 mmol) $NaBH_4$ dissolved in 45 mL water and thermostated at 25.0 ± 0.1 °C. The initial concentration of **1** in the reaction solution was 2.0 mM and concentration of $P(OMe)_3$ was 8.0 mM. The reaction was started by turning on the stirrer at 1000 rpm under inert atmosphere. The hydrogen evolved during the reaction was collected over water in the graduated glass column. After 6 h stirring, when no more hydrogen was evolved, the mixture was extracted with dichloromethane and the combined organic extracts were cooled in order to precipitated some traces of sodium borohydride or metaborate remaining in organic extracts. Then, the solution was dried over magnesium sulfate, filtered and evaporated in vacuo giving a residue containing mainly unreacted **1** and **3** complexes. The residue was dissolved in cold hexane and due to lower solubility in hexane, **1** was precipitated and separated by filtration. Evaporation of hexane in vacuo gives pure **3**. Colorless crystals of **3** were obtained by the crystallization from hexane at 0 °C after 10 days (19.2 mg, 33%). Complex **3**: ^1H NMR ($CDCl_3$, ppm): δ −5.71 (br s, 2H, Ru—H), 3.45 (br m, 18H, $POCH_3$), 3.47 (d, J = 4.4 Hz, 18H, $POCH_3$). ^{13}C NMR ($CDCl_3$, ppm): δ 49.32, 49.8. ^{31}P NMR ($CDCl_3$, ppm): δ 169.65, 172.4. Mass: m/z 597 ($[M-2H]^+$, 100%), 473($[M-P(OMe)_3H_2]^+$, 38%). UV: λ_{max} (THF, nm) (ε in $dm^3\ mol^{-1}\ cm^{-1}$) 295 (52,500). FTIR (KBr, υ, cm^{-1}): 2928 m, 1580–1720 m, 1445 w, 1375 w, 1066 s.

2.4. Single crystal X-ray diffraction analysis of 3

Colorless, prismatic crystal of dimension 0.3 mm × 0.2 mm × 0.2 mm was glued to thin quartz glass and mounted on the goniometry of Enraf Nonious CAD4 diffractometer at room temperature. A hemisphere data was collected in $\omega/2\theta$ scan mode with graphite monochromated Mo Kα radiation, λ = 0.71073 Å. Data collection and initial indexing were handled using XCAD4 [14]. Semi-empirical absorption corrections were performed using PSI-SCANS [15]. The structure was solved using direct method and difference Fourier technique. Hydrogen atoms of the methyl groups were attached via the riding model. Hydrogen atoms on the Ru atoms were taken from a difference Fourier map and fixed all parameters after applied some restraints. The final structural refinement included anisotropic temperature factors on all non-hydrogen atoms. Structure solution, refinement, graphics, and creation of publication material were performed using SHELX [16] and WinGX package [17]. Graphical representations of the structure was made with MERCURY [18]. CCDC file 781525 contains the supplementary crystallographic data for this paper. These data can be obtained free of charge from The Cambridge Crystallographic Data Center via www.ccdc.cam.ac.uk/data_request/cif.

2.5. Catalytic activity of 3 in the hydrolysis of sodium borohydride

A catalyst solution was prepared by dissolving 18 mg (0.030 mmol) **3** in a mixture of 5 mL THF and 5 mL water under vigorous stirring. In a separate glass vial, 852 mg (22.5 mmol) $NaBH_4$ was dissolved in 40 mL water and the solution was transferred into the reaction flask thermostated at 25.0 ± 0.1 °C. Then, the catalyst solution in 10 mL THF/water was also transferred into the reaction flask, yielding a solution with ruthenium concentration of 0.60 mM and SB concentration of 450 mM. The experiment was started by closing the reaction flask and turning on the stirring at 1000 rpm simultaneously. The volume of hydrogen gas evolved was measured by recording the displacement of water level in the graduated glass tube for every 5 min.

2.6. UV–vis spectroscopic measurements during hydrolysis of sodium borohydride catalyzed by **1** and $P(OMe)_3$

A stock solution of $P(OCH_3)_3$ (100 mM) in THF was prepared by dissolving 1.18 mL $P(OCH_3)_3$ (MW = 124.08 g/mol, d = 1.052 g/mL) to 100 mL THF. For the preparation of catalyst solution with $P(OCH_3)_3$/**1** ratio of 2–4, an aliquot of the stock solution (2–4 mL) was diluted to 5 mL by adding THF and, then, 40 mg **1** was added to this solution and dissolved completely by stirring the solution. Then, the solution was transferred into the reaction flask containing 852 mg (22.5 mmol) $NaBH_4$ dissolved in 45 mL water and thermostated at 25.0 ± 0.1 °C. The initial concentration of **1** in the reaction solution was 2.0 mM and concentration of $P(OCH_3)_3$ was in the range of 4.0–8.0 mM. The reaction was started by turning on the stirrer at 1000 rpm under inert atmosphere. The hydrolysis of SB catalyzed by different ratio of $P(OCH_3)_3$/**1**, was followed by taking the UV–vis absorption spectra. Every 10 min, 50 μL aliquot was taken from the reaction solution with a micropipette and diluted to 3 mL with SB solution (450 mM) in H_2O–THF (9:1). UV–vis spectrum of the diluted solution was taken immediately.

2.7. Isolation of catalytically active ruthenium(II) species stabilized by 2,2′-bipyridine in the form of complex **4**

For the preparation of catalyst solution with $P(OCH_3)_3$/**1** ratio of 3, a 3.0 mL aliquot of the stock solution of $P(OCH_3)_3$ (100 mM) in THF was diluted to 5 mL by adding THF and, then, 40 mg **1** was added to this solution and dissolved completely by stirring. Then, the solution was transferred into the reaction flask containing 852 mg (22.5 mmol) $NaBH_4$ dissolved in 45 mL water and thermostated at 25.0 ± 0.1 °C. The initial concentrations of **1** and $P(OCH_3)_3$ in the reaction solution were 2.0 and 6.0 mM, respectively. The reaction was started by turning on the stirrer at 1000 rpm under inert atmosphere. After about 1 h stirring (induction time), active catalyst was formed accompanied by a sudden increase in the hydrogen generation rate. Changes in the catalyst were followed by taking UV–vis spectra. Immediately after induction period, when the active catalyst was in situ formed, 2,2′-bipyridine (20 mg, 0.13 mmol) was added to the reaction solution. It was stirred for additional 5 h at 25.0 ± 0.1 °C under inert atmosphere. During that time, the color of solution changed from red to red-brown and finally to dark-brown. Then, the mixture was extracted with dichloromethane and the combined organic extracts were cooled to 0 °C, whereby traces of SB or metaborate remaining in organic extracts were precipitated out. Then, the solution was dried over magnesium sulfate, filtered and evaporated in vacuo giving a residue containing mainly the complex **4** and some traces of 2,2′-bipyridine. The latter was easily removed from the complex by washing with cold hexane. Recrystallization from a mixture of chloroform–hexane solution yields the complex (21.7 mg, 45%). Complex **4**: ^{1}H NMR ($CDCl_3$, ppm): δ −5.59 (s, 1H, Ru—H), 1.45 (br, 6H, CH_3), 3.42 (s, 9H, OCH_3), 6.45 (m, 4H, H-bipy), 6.99 (m, 4H, H-bipy). ^{13}C NMR ($CDCl_3$, ppm): δ 40.5, 50.91, 100.02, 125.6, 127.8, 145.18. ^{31}P NMR ($CDCl_3$, ppm): δ 163.22. Mass: m/z 456 ([M−2C]$^+$, 100%). UV: λ_{max} (THF/H_2O, nm) (ε in dm^3 mol^{-1} cm^{-1}) 235 (12,400), 285 (36,500), 460 (4500). FTIR (KBr, υ, cm^{-1}): 1490–1550 s.

2.8. Catalytic activity test and UV–vis spectroscopic measurements during catalytic hydrolysis of sodium borohydride starting with **1** and 3 equiv. $P(OCH_3)_3$ plus 2,2′-bipyridine added

A stock solution of $P(OCH_3)_3$ (100 mM) in THF was prepared by dissolving 1.18 mL $P(OCH_3)_3$ (MW = 124.08 g/mol, d = 1.052 g/mL) to 100 mL THF. For the preparation of catalyst solution with $P(OCH_3)_3$/**1** ratio of 3, an aliquot of the stock solution (3 mL) was diluted to 5 mL by adding THF and, then, 40 mg **1** was added to this solution and dissolved completely by stirring. Then, the solution was transferred into the reaction flask containing 852 mg (22.5 mmol) $NaBH_4$ dissolved in 45 mL water and thermostated at 25 °C. The initial concentrations of **1** and $P(OCH_3)_3$ were 2.0 and 6.0 mM, respectively. The experiment was started by closing the reaction flask and turning on the stirring at 1000 rpm simultaneously. The volume of hydrogen gas evolved was measured by recording the displacement of water level in the graduated glass tube for every 5 min. After about 1 h stirring (induction time), when a fast hydrogen evolution started, 20 mg (0.127 mmol) 2,2′-bipyridine was added to reaction solution at 25 °C under inert atmosphere. Then, the volume of hydrogen gas evolved was further measured every 5 min (for additional 4 h).

This experiment was repeated starting with 40 mg **1** (2 mM), 852 mg $NaBH_4$ (450 mM), 20 mg (2.5 mM) 2,2′-bipyridine and a $P(OCH_3)_3$/**1** ratio of 3 (6 mM of phosphine) in 50 mL H_2O–THF. The reaction was followed by taking UV–vis absorption spectra. Every 10 min, a 50 μL aliquot was taken with a micropipette and diluted to 3 mL with $NaBH_4$ solution (450 mM) in H_2O–THF (9:1).

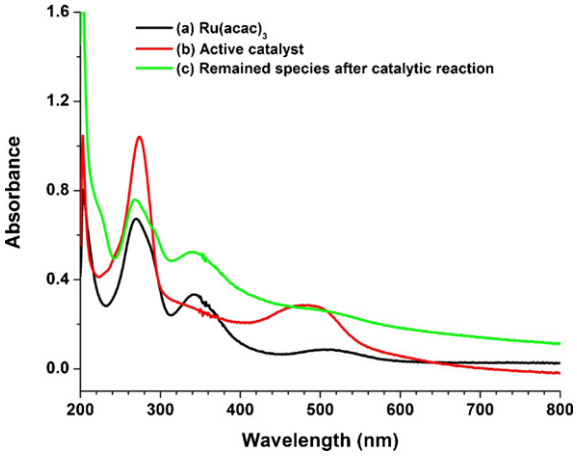

Fig. 1. UV–vis electronic absorption spectra taken from the reaction solution during the hydrolysis of sodium borohydride started with $NaBH_4$ (450 mM), complex **1** (2 mM) and $P(OMe)_3$ (4–8 mM) in THF–H_2O (1:9) at 25 °C.

3. Results and discussion

When trimethylphosphite, $P(OMe)_3$, is added to the reaction solution containing 450 mM $NaBH_4$ and 2 mM 1 in 50 mL H_2O–THF solution, the hydrogen generation is practically ceased (or reduced to the level of self-hydrolysis of SB). However, the catalytic hydrolysis of SB restarts at an unexpectedly high rate after a certain period (induction time) [8]. When **1** is used alone as a homogeneous catalyst, the turnover frequency (TOF) is 4.7 min^{-1} (the rate of hydrogen generation is 11 mL H_2/min), while in the presence of 2 equiv. trimethylphosphite the TOF value is 37 min^{-1} (hydrogen generation rate becomes 83 mL H_2/min) after induction time. Moreover, the total turnover number (TTON) of sole **1** in the catalytic hydrolysis of SB is 1200 (over 3 h) [1], while the TTON of **1** in the presence of 2 equiv. trimethylphosphite is 20,700 (over 72 h) [8]. This comparison indicates the formation of a new ruthenium catalyst containing phosphine ligands, which is much more active and has longer lifetime than that of the parent ruthenium complex in the hydrolysis of SB. The challenge here is to find out what the active catalyst is in this system.

Monitoring the UV–vis electronic absorption spectra during the catalytic hydrolysis of SB starting with **1** and $P(OMe)_3$ gives some insights into the nature of active catalyst. Fig. 1 displays three UV–vis absorption spectra taken at different stages of the catalytic reaction. The spectrum taken from the mixture before the

reaction (before adding SB, Fig. 1a) shows three prominent absorption bands at 270, 350 and 509 nm assigned to charge transfer transitions and d–d transition of **1**, respectively [19]. UV–vis spectrum taken from the reaction solution after induction period (Fig. 1b) exhibits one absorption band at 480 nm with higher intensity compared to that of **1** and another band at 275 nm. These two bands remain during the whole reaction and should be due to the active catalyst **2**. The spectrum taken at the end of the catalytic reaction (Fig. 1c) shows essentially the same absorption features as the ones of **1** before the reaction. This observation indicates that the active catalyst **2** is alive during the catalysis, but converted to the parent **1** when the hydrolysis of SB is over. The UV–vis spectrum observed for **2** during the catalytic reaction (Fig. 1b) resembles the electronic absorption spectra of three octahedral ruthenium(II) complexes known in literature: $[Ru(en)2IP]^{2+}$, $[Ru(en)Phen]^{2+}$, (IP: imidazo[4,5-f][1,10]phenanthroline and Phen: 1,10 – phenanthroline) [20] and cis-$[Ru(acac)_2\{P(OMe)_3\}_2]$ [9]. This implies that the active catalyst is most likely a ruthenium(II) species. That the active catalyst is alive as long as hydrogen generation continues, i.e. as long as SB is present in solution, leads to a long catalytic lifetime (vide infra). However, the active catalyst decomposes immediately when the hydrogen generation stops, i.e. no more SB in the catalytic solution is left, forming the parent complex **1**. The presence of the parent complex **1** was confirmed by the ^1H and ^{13}C NMR spectra of the crude organic extract obtained from the solution after the catalytic reaction. It is noteworthy that performing the same catalytic hydrolysis starting with different ratios of $P(OMe)_3$ to **1** in the range of 1–4 gives the same UV–vis electronic absorption spectra indicating that changing the ratio of $P(OMe)_3$ to **1** does not affect the structure of active catalyst or mechanism of catalytic hydrolysis of SB. In order to identify the true active catalyst formed in situ from **1** and $P(OMe)_3$ under the reducing conditions, **2** had to be isolated. When the catalytic hydrolysis of SB was completed (no more hydrogen evolution), the mixture was extracted with dichloromethane. The ^1H NMR spectrum of the crude organic extract gives an intense peak at −5.66 ppm for **1**. So does the ^{13}C NMR spectrum show a broad intense signal at −23.5 ppm for the paramagnetic complex **1**. ^1H and ^{13}C NMR spectra of the crude extract show additionally weak signals at 3.48 and 50.9 ppm, respectively, attributable to the $P(OMe)_3$ ligands of a complex in small amount in the sample. The insoluble

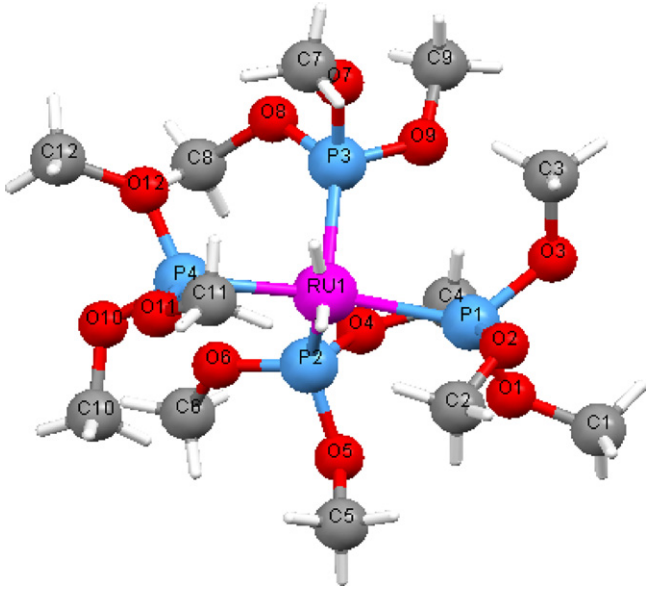

Fig. 2. X-ray crystal structure of complex **3**.

1 could be precipitated out from the hexane solution of the crude extract. Colorless crystals of a ruthenium complex were obtained upon cooling the hexane solution at 0 °C after 10 days and characterized to be dihydridotetrakis(trimethylphosphite)ruthenium(II), **3**.

Single crystals of **3** were used for the XRD structure determination. Crystal data and experimental details of the title compound plus the average values of selected bond lengths and angles are given in Tables 1 and 2 in the Supporting information, respectively. The complex crystallizes in the triclinic space group P-1 with three asymmetric unit formula of **3** in the unit cell (Fig. 2). Projection of the crystal structure of the complex **3** involving a unit cell with three asymmetric molecules and three inversion symmetry related molecules is shown in Fig. S1 in the supporting information. The coordination around the Ru atom involves four P atoms of the $P(OMe)_3$ ligands and two H atoms. The four P—Ru—P bond angles within the coordination sphere are in the range of 96.3(2)–101.1(3)°, the other two P—Ru—P bond angles are in the range of 153.67(19)–155.2(2)°. Two H atoms locate at the wide angle position in the coordination sphere. The average bond distances for three molecules of the complex are Ru1-P = 2.268, Ru2-P = 2.264 and Ru3-P = 2.265 Å (Table 2 in the supporting information). The mean Ru—P bond length in **3** is 2.265 Å which is comparable to the corresponding bond lengths of 2.259 Å in carbonyl($^5\eta$-cyclopentadienyl)-bis(trimethylphosphite)ruthenium(II) ion [21], 2.221 Å in bis(π-2-methylallyl) bis(trimethylphosphite)ruthenium [22], and 2.206 Å in cis–bis(acetylacetonato)bis(trimethylphosphite)ruthenium(II) [9]. However, it is shorter than those of complexes containing trimethylphosphite ligands in two trans positions such as trans–bis(acetone-hydrazone)tetrakis(trimethylphosphite)ruthenium(II) ion (a mean Ru—P distance is 2.35 Å) [23] or trans–bis(acetylacetonato)bis(trimethylphosphite)-ruthenium(II) (an average Ru—P distance of 2.317 Å) [9].

The solution NMR data of **3** are also in agreement with the single crystal structure. The ^1H NMR spectrum taken from chloroform-d solution gives two signals for the $P(OMe)_3$ groups at 3.45 and 3.47 ppm and a singlet at −5.71 ppm for the hydrido ligands. The ^{13}C NMR spectrum gives two singlets at 49.32 and 49.80 ppm for the $P(OMe)_3$ groups. The ^{31}P NMR spectrum gives two separate peaks at 169.65 and 172.4 ppm which can be assigned to the two $P(OMe)_3$ ligands trans to each other and the two other $P(OMe)_3$ ligands trans to hydrido ligands (or cis to each other), respectively. Note the small differences in chemical shifts of $P(OMe)_3$ ligands indicating that the geometry is a highly distorted octahedral. The phosphorus atoms in **3** are less shielded compared to the ones in $[Ru\{P(OMe)_3\}_4Cl_2]$ (131 ppm) [24], where two chloro ligands put electron density on the central metal ion more than that two hydride ligands can do.

UV–vis electronic absorption spectrum of **3** shows a very intense absorption band at 295 nm, assigned to a charge transfer transition and clearly different from the one observed for the Ru(II) species **2**, in situ formed and exists in solution during the catalytic hydrolysis of SB (Fig. 1b). Mass spectrum of **3** (Fig. S2 in the supporting information) shows $[M-2H]^+$ peak at $m/z = 597$ along with another peak at $m/z = 473$ for the $[M-P(OMe)_3H_2]^+$ fragment. The simulated spectrum with the isotope distribution fits well to the experimentally observed isotope pattern for the molecular peak (Fig. S2 in the supporting information).

The UV–vis electronic absorption spectra taken from the solution during the catalytic hydrolysis of SB starting with **1** and $P(OMe)_3$ indicates the existence of a ruthenium(II) species which is most likely the active catalyst. This ruthenium(II) species **2** decomposes immediately after completion of the hydrolysis of SB, forming mostly **1** and very small amount of **2** is converted to the stable

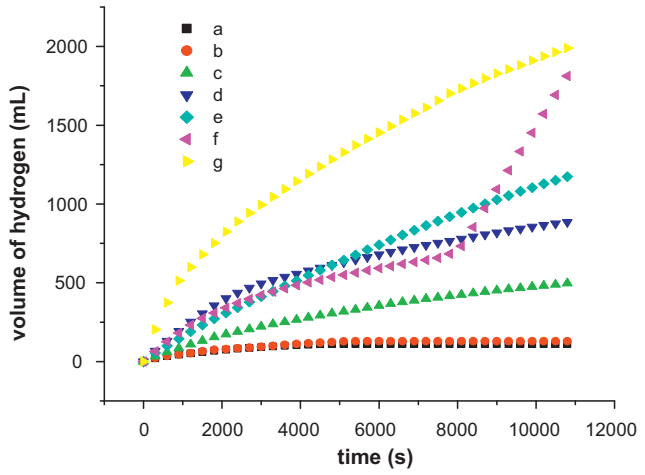

Fig. 3. Volume of H_2 versus time for the hydrolysis of $NaBH_4$ using compounds: (a) cis-[Ru(acac)$_2${P(OMe)$_3$}$_2$], (b) trans-[Ru(acac)$_2${P(OMe)$_3$}$_2$], (c) trans-[Ru(acac)$_2${P(OMe)$_3$}$_2$] plus 2 equiv. of P(OMe)$_3$, (d) complex **3**, (e) complex **1**, (f) complex **1** plus 2 equiv. of P(OMe)$_3$, (g) cis-[Ru(acac)$_2${P(OMe)$_3$}$_2$] plus 2 equiv. of P(OMe)$_3$.

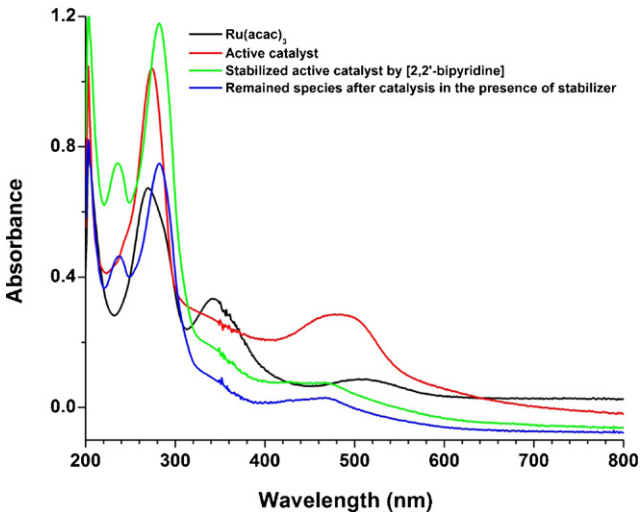

Fig. 4. UV–vis spectroscopic measurements during hydrolysis of $NaBH_4$ (450 mM) starting with 2 mM **1** and 3 equiv. of P(OMe)$_3$ along with stabilization by 2,2′-bipyridine (2.5 mM).

ruthenium(II) complex **3** as a minor product which could be isolated.

The complex **3** was employed as homogeneous catalyst in the hydrolysis of SB. Fig. 3 shows the plots of hydrogen volume generated versus time during the hydrolysis of SB starting with one of **3**, **1**, trans- or cis-[Ru(acac)$_2${P(OMe)$_3$}$_2$] [9] complexes with/without 2 equiv. of trimethylphosphite. Using **3** as catalyst gives activity in the hydrolysis of SB, comparable to that of **1** [8] or cis-[Ru(acac)$_2${P(OMe)$_3$}$_2$] [9], but definitely much lower than that obtained by using **1** plus 2 equiv. of P(OMe)$_3$. Taking all the results together one can conclude that **3** is not the active catalyst, rather formed from the active catalyst when the hydrogen generation (reducing condition) is over.

Since the in situ formed ruthenium(II) species acting as catalyst in the hydrogen generation from the hydrolysis of SB starting with **1** and P(OMe)$_3$ could not be isolated from the reaction solution, we attempted to stabilize this active catalyst by adding a chelating ligand such as 2,2′-bipyridine (bipy) into the reaction solution during catalytic reaction. For this purpose, a catalytic reaction was started with 2.0 mM of 1, 6.0 mM P(OMe)$_3$ and 450 mM $NaBH_4$ in 50 mL H_2O–THF at 25 °C and was followed by taking UV–vis spectra and measuring the volume of hydrogen gas generated. After an induction time of 1 h, the active catalyst is formed in situ as seen from the UV–vis spectrum (Fig. 4) and a fast hydrogen generation starts concomitantly. At that point, 2,2′-bipyridine (2.5 mM) was quickly added into the reaction solution and the reaction was followed further by UV–vis spectra (Fig. 4). Upon addition of bipy, there is an observable change in the UV–vis spectrum, now giving three absorption bands at 235, 285 and 460 nm indicating that the active catalyst is changed. Also a simultaneous change is observed in the rate of hydrogen generation (see later). The new absorption features remain not only throughout the catalytic reaction but also after the hydrolysis, indicating that the new complex, formed upon addition of bipy, is indeed stable and can be isolated. The isolation of the complex stabilized by bipy was achieved by extraction from the reaction solution with dichloromethane. Recrystallization from chloroform–hexane mixture gives a complex as crystalline powder which was characterized to be complex **4**. The ^{1}H NMR spectrum of **4** in chloroform-d solution gives a singlet at −5.59 ppm for the hydride, a broad peak at 1.45 ppm for the methyl groups of acetylacetonato ligand, a singlet at 3.42 ppm for the trimethylphosphite ligand and two multiplets at 6.45 and 6.99 ppm for the hydrogens of 2,2′-bipyridine ligand. The ^{13}C NMR spectrum gives a peak at 40.5 ppm for methyl carbons of acetylacetonato ligand, a singlet at 50.91 ppm for the trimethylphosphite ligand, a singlet at 100.02 ppm for the methine carbon of acac ligand, signals at 125.6–127.8 ppm for the carbons of bipy and one doublet at 145.18 ppm for the carbonyls of acac ligand. ^{31}P NMR spectrum of **4** shows a single peak at 163.22 ppm. Mass spectrum of **4** (Fig. S3 in the supporting information) shows a peak at m/z = 456 for the fragmented ion [Ru(bipy){P(OMe)$_3$}(OCH$_2$CH$_2$CH$_2$O)]$^+$. The spectrum simulated for the $C_{16}H_{23}O_5N_2P_1Ru_1$ with isotopic distribution exactly matches the experimentally observed isotope pattern of this fragmentation peak.

Regarding the formation of **4**, the bidentate bipy might have replaced either one acac ligand in a putatively active catalyst or two monodentate trimethylphosphite ligands. To obtain a clue which one of these two possible ligand replacements is the actual process, we performed a catalytic test reaction starting with **1**, $NaBH_4$ and 2,2′-bipyridine, that is, without using trimethylphosphite, and followed by taking UV–vis electronic absorption spectra. After 24 h, no change was observed in the UV–vis electronic absorption spectrum. This observation indicates that acac ligands in the ruthenium complex cannot be replaced directly by bipy even after a very long time in the presence of SB. Rationally, one can conclude that two trimethylphosphite ligands are replaced by one bipy ligand forming complex **4** from the active catalyst. Consequently, we can suggest the active catalyst **2** to be [Ru(acac){P(OMe)$_3$}$_3$H] or one of its dissociation products. The observation of a ruthenium(II) species in solution during the catalytic hydrolysis of SB (Fig. 1) supports this suggestion. That the catalytic activity of cis-[Ru(acac)$_2${P(OMe)$_3$}$_2$] in the hydrolysis of $NaBH_4$ is significantly enhanced by addition of trimethylphosphite into the medium [9] is another piece of evidence supporting the presence of such a complex. That the catalytic activity of trans-[Ru(acac)$_2${P(OMe)$_3$}$_2$] is much lower than that of the cis-isomer in the presence of trimethylphosphite [9] leads to conclusion that the active catalyst has three phosphorus ligands in a facial arrangement. Upon reaction with trimethylphosphite, trans-[Ru(acac)$_2${P(OMe)$_3$}$_2$] can yield only a complex with meridional arrangement of three phosphorus ligands, in which the ruthenium center is sterically less accessible for the substrate, than that in the facial isomer, fac-**2**. Moreover, the stable ruthenium(II) species **3**, isolated from the reaction solution after catalysis, contains four bulky trimethylphosphite ligands and, therefore, is sterically less favorable to act as an active catalyst in comparison with fac-**2** complex.

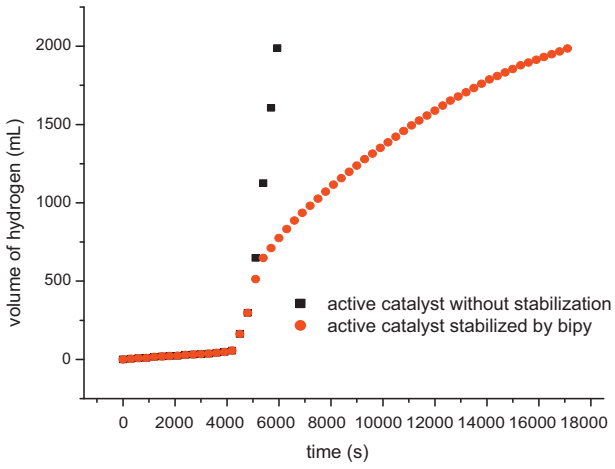

Fig. 5. Volume of H_2 versus time plots for the hydrolysis of $NaBH_4$ (450 mM) starting with **1** (2 mM) and 3 equiv. of $P(OMe)_3$ in the absence of 2,2′-bipyridine (black squares) and in the presence of 2,2′-bipyridine (2.5 mM) added after induction period (red circles). (For interpretation of the references to color in this figure legend, the reader is referred to the web version of the article.)

It is noteworthy to compare the catalytic activity of **2** with that of the bipy-stabilized complex **4**. Fig. 5 shows the hydrogen evolution versus time plots for the hydrolysis of SB starting with **1** and $P(OMe)_3$ in the absence or presence of 2,2′-bipyridine added after induction period. The rate of hydrogen generation decreases from 83 mL H_2/min for the in situ active catalyst down to 8 mL H_2/min upon adding 2,2′-bipyridine.

Taking all the results together reveals that fac-**2** or one of its dissociation products is most likely the active catalyst **2** in the hydrolysis of SB starting with **1** and $P(OMe)_3$. This 18-electron ruthenium(II) complex can hardly bind a substrate molecule to start the catalytic cycle. However, it can readily undergo detachment of one $P(OMe)_3$ ligand generating temporarily the coordinatitvely unsaturated, 16-electron ruthenium(II) complex, $[Ru(acac)\{P(OMe)_3\}_2H]$, which is at equilibrium with the dominant parent complex fac-**2**. The latter complex can be in situ formed from either **1** or cis-$[Ru(acac)_2\{P(OMe)_3\}_2]$ in the presence of $P(OMe)_3$ during the catalytic hydrolysis of SB. The catalytically active species, $[Ru(acac)\{P(OMe)_3\}_2H]$ and fac-**2**, are alive, at equilibrium with each other, only under reducing conditions, as long as SB is present in the medium. However, they are converted to stable compounds when no more SB is present in solution. Since the UV–vis spectrum shows the absence of **1** in the solution during catalysis, the complex **1** recovered after the catalytic reaction must be formed from the active catalyst when the reducing condition is over. As there exist free trimethylphosphite in the reaction solution, a small fraction of the active catalyst is also converted to **3**. In the light of present information, it is not possible to write a stoichiometric equation for the conversion of active catalyst to **1** and **3** or any other minor product as free acetylacetonate and trimethylphosphite are likely involved in this conversion.

4. Conclusion

In summary, our study on the catalytic system comprising **1** plus $P(OMe)_3$ in the hydrolysis of $NaBH_4$ leads to the following conclusions and insights, some of which were previously unavailable: (i) An active catalyst is in situ formed temporarily during hydrolysis of $NaBH_4$ starting with **1** and $P(OMe)_3$. (ii) The active catalyst which is a ruthenium(II) species is alive as long as the hydrogen generation continues, i.e., sodium borohydride is present in the catalytic solution. (iii) After the catalytic reaction, when no more hydrogen is generated, the active catalyst decomposes forming mostly ruthenium(III) acetylacetonate (**1**), along with stable ruthenium(II) complex containing four trimethylphosphite ligands, **3**, as a minor product. (iv) The active catalyst can be stabilized by 2,2′-bipyridine and isolated from the catalytic reaction solution as complex **4**. (v) The active catalyst is most likely a coordinatively unsaturated, 16-electron ruthenium(II) complex, $[Ru(acac)\{P(OMe)_3\}_2H]$, which is generated by detachment of a $P(OMe)_3$ ligand from the 18-electron fac-**2** complex. The latter can be generated not only from **1** but also from cis-$[Ru(acac)_2\{P(OMe)_3\}_2]$ in the presence of trimethylphosphite during the hydrolysis of sodium borohydride. (vi) fac-**2** is sterically more favorable to act as homogeneous catalyst to produce hydrogen in comparison with its meridional form or complex **3** containing four bulky ligands. (vii) The active catalyst has much higher catalytic activity in comparison with its form stabilized by 2,2′-bipyridine.

Acknowledgements

Partial support of this work by Turkish Academy of Sciences and TUBITAK (Project No.: 105M357) is gratefully acknowledged. M.M. thanks TUBITAK for awarding a PhD fellowship. We thank Mr. Bunyamin Cosut from Gebze Institute of Technology for performing mass analysis.

Appendix A. Supplementary data

Supplementary data associated with this article can be found, in the online version, at doi:10.1016/j.molcata.2011.12.015.

References

[1] E. Keceli, S. Özkar, J. Mol. Catal. A: Chem. 286 (2008) 87.
[2] A. Zuttel, Naturwissenschaften 91 (2004) 157.
[3] S.C. Amendola, P. Onnerud, M.T. Kelly, P.J. Petillo, G.L. Sharp, M. Binder, J. Power Source 85 (2000) 186.
[4] S.C. Ammendola, J.M. Janjua, N.C. Spencer, M.T. Kelly, P.J. Petillo, G.L. Sharp, M. Binder, Int. J. Hydrogen Energy 25 (2000) 969.
[5] J.Y. Lee, H.H. Lee, J.H. Lee, D.M. Kim, J.H. Kim, J. Electrochem. Soc. 149 (2002) 603.
[6] H.I. Schlesinger, H.C. Brown, A.B. Finholt, J.R. Gilbreath, H.R. Hockstra, E.K. Hydo, J. Am. Chem. Soc. 75 (1953) 215.
[7] U.B. Demirci, O. Akdim, P. Miele, J. Power Sources 192 (2009) 310.
[8] M. Masjedi, T. Demiralp, S. Özkar, J. Mol. Catal. A: Chem. 310 (2009) 59.
[9] M. Masjedi, L.T. Yildirim, S. Ozkar, Inorg. Chim. Acta 363 (2010) 1713.
[10] M.A. Bennett, G. Chung, D.C.R. Hockless, H. Neumann, A.C. Willis, J. Chem. Soc. Dalton Trans. (1999) 3451.
[11] M.A. Bennett, M.J. Byrnes, A.C. Willis, Dalton Trans. (2007) 1677.
[12] D.H. Gerlach, W.G. Peet, E.L. Muetterties, J. Am. Chem. Soc. 94 (1972) 4545.
[13] M. Zahmakiran, S. Özkar, J. Mol. Catal. A: Chem. 258 (2006) 95.
[14] XCAD4: K. Harms, S. Wocadlo, XCAD4, University of Marburg, Germany, 1995.
[15] A.C.T. North, D.C. Phillips, F.S. Mathews, Acta Crystallogr. A 24 (1968) 351.
[16] SHELX: G.M. Sheldrick, Acta Crystallogr. A 64 (2008) 112.
[17] WinGX: L.J. Farrugia, J. Appl. Crystallogr. 32 (1999) 837.
[18] MERCURY: C.F. Macrae, P.R. Edgington, P. McCabe, E. Pidcock, Shields G.P., R. Taylor, M. Towler, J. Van de Streek, J. Appl. Crystallogr. 39 (2006) 453.
[19] R. Grobelny, B. Jezowska-Trzebiatowska, W. Wojciechowski, J. Inorg. Nucl. Chem. 28 (1966) 2715.
[20] P. Nagababu, J.N.L. Latha, S. Satyanarayana, Chem. Biodivers. 3 (2006) 1219.
[21] K.G. Frank, J.P. Selegue, Acta Crystallogr. C 47 (1991) 35.
[22] R.A. Marsh, J. Howard, P. Woodward, J. Chem. Soc. Dalton (1973) 78.
[23] M.J. Nolte, E. Singleton, J. Chem. Soc. Dalton (1974) 2406.
[24] N.S. Goncalves, S.E. Mazzetto, Transit. Met. Chem. 27 (2002) 646.